

# Spectral Analysis of Correlated One-Dimensional Systems with Impurities

Stephan Haas

*Theoretische Physik, ETH-Hönggerberg, CH-8093 Zurich, Switzerland*  
(January 21, 2022)

An averaging procedure is proposed to account for spectral features of correlated one-dimensional systems in the presence of non-magnetic impurities. The dynamical spin structure factor for a corresponding random ensemble of Heisenberg chain segments is calculated by exact numerical diagonalization. It is shown that a few-pole approximation is sufficient to describe the numerical results. A similar analysis is proposed for the discussion of experimental spectra, such as obtained by inelastic neutron scattering measurements on Zn-doped CuO chains. By examination of the disorder-induced pseudo-gap, the loss of spectral weight, and the discrete peak structures due to smallest-cluster contributions, the underlying impurity distribution function can be determined.

It is known that electrons in one dimension are localized by an infinitesimal amount of disorder. [1] Analogously, their spin degrees of freedom develop a spectral gap when impurities are placed into an infinite chain. The branch cut corresponding to the collective spinon continuum of the pure system splits into a discrete set of poles characterized by conformal towers of excitations, and the spacing between the poles in a given one-dimensional segment decreases with increasing size. In this paper it is proposed that an average over a distribution of one-dimensional segments, defined by the regions between randomly placed impurities, should be taken when calculating physical quantities. At low energies, the finite system gaps of all contributing segments then add up to form a pseudo-gap. By analyzing the peak structure, the overall spectral weight, and the pseudo-gap features of quasi-one-dimensional crystals in the presence of non-magnetic impurities, such as Zn-doped CuO chains [2] and non-stoichiometric  $\alpha'$ - $\text{NaV}_2\text{O}_5$ , [3] the respective distribution function of lengths of chain segments can thus be deduced, indicating the extent to which the introduction of defects has pushed the system into a mesoscopic regime.

As a non-trivial paradigm for correlated one-dimensional systems, let us thus focus on the antiferromagnetic spin-1/2 Heisenberg chain in the presence of non-magnetic impurities. Such a model is realized for example in Zn-doped  $\text{SrCuO}_2$ , where the antiferromagnetic superexchange between neighboring  $\text{Cu}^{2+}$   $d_{x^2-y^2}$  electrons is mediated by the filled  $\text{O}^{2-}$  p-orbitals. By substituting  $\text{Zn}^{2+}$  for  $\text{Cu}^{2+}$ , static vacancies are created, and the infinite chain is separated into segments of length  $l$  which follow a distribution function  $P(l)$ .

The dynamical structure factor  $S(q, \omega)$  of the infinite antiferromagnetic spin-1/2 Heisenberg chain is described approximately by a two-spinon continuum of excitations which can be probed by inelastic neutron scattering experiments. [4] It is bounded from below by the des Cloiseaux-Pearson dispersion,  $\omega_1(q) = (\pi J/2)|\sin(q)|$ , [5] and from above by the maximum energy of two unbound spinons  $\omega_2(q) = \pi J|\sin(q/2)|$ . [6] Thus at  $q=\pi$  the two spinons have maximal phase space, and the dynamical

structure factor diverges as  $S(\pi, \omega) \sim (1/\omega)\ln(1/\omega)$  at the lower boundary. [6,7] For finite systems with an even number of sites,  $l$ , the corresponding branch cut splits into a discrete set of  $l/4$  poles for  $l=4, 8, 12, \dots$ , and  $(l+2)/4$  poles for  $l=2, 6, 10, \dots$  (see Fig. 1(a)). Chains with an odd number of sites do not contribute at  $q=\pi$ . [8] The finite-size scaling behavior of the pole positions, shown in Fig. 1(b), is well described by the towers of excitations found in conformal field theory (CFT), when logarithmic corrections due to marginally relevant operators are taken into account. [9–11] Thus the pole positions are of the form

$$\omega_i(l) = \alpha_i/l + \beta_i/(l \ln(l)), \quad (1)$$

where  $\alpha_i$  and  $\beta_i$  are treated as fit parameters.

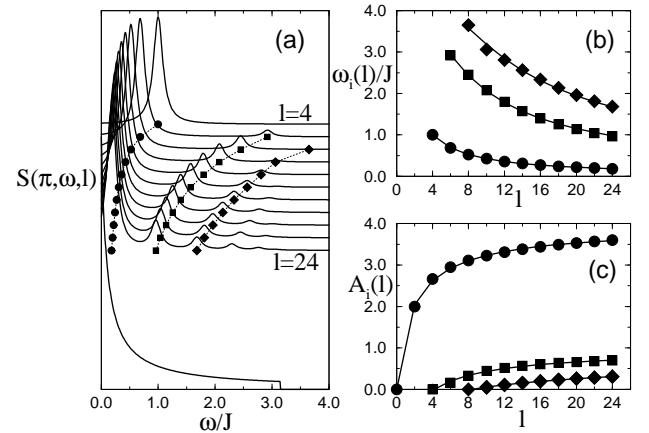


FIG. 1. (a) Finite-size scaling of the  $q=\pi$  dynamical structure factor of the antiferromagnetic spin-1/2 Heisenberg chain. In the thermodynamic limit ( $l = \infty$ ) the discrete set of poles merges into a single branch cut. The  $\delta$ -peaks have been given a width of  $\epsilon=0.1J$ . (b) Finite-size scaling of the first three pole positions in (a). (c) Finite-size scaling of the corresponding pole weights. The solid lines in (b) and (c) are fits to the finite cluster data discussed in the text.

In Fig. 1(b), the first three pole positions for finite-size clusters up to  $l=24$  (symbols) are shown along with the fits to Eq. 1 (solid lines). There is good agreement of  $\alpha_i$

with the predictions from CFT, [9] e.g.  $\alpha_1^{CFT} = \pi^2 J/2$ , while the fit yields  $\alpha_1 = 4.614J \approx 0.94\alpha_1^{CFT}$ .

The pole positions may be calculated directly from the Bethe Ansatz equations or approximately using CFT, whereas their respective matrix elements are accessible only to numerical diagonalizations of small clusters. In Fig. 1(c) it is shown that a fit of the finite cluster pole weights,  $A_i(l)$ , to the form

$$A_i(l) = a_i + b_i \ln(1+l) + c_i \ln(1 + \ln(1+l)), \quad (2)$$

gives good results, and thus permits extrapolation to larger system sizes. The dynamical spin structure factor at  $q=\pi$  for a system of length  $l$  can then be written in the form

$$S(\pi, \omega, l) = \sum_i A_i(l) \delta(\omega - \omega_i(l)), \quad (3)$$

where the sum is taken over all poles. In practice, the  $\delta$ -peaks are replaced by Lorentzians of width  $\epsilon$ , which throughout this paper will be taken as  $\epsilon = 0.1J$ .

Let us now turn to the effect of vacancies entering an ideal infinite chain i.e. by doping the system with non-magnetic impurities. Even mobile carriers which can be introduced into the chain by out-of-plane substitutions (such as  $\text{La}^{3+}$  for  $\text{Sr}^{2+}$  in  $\text{SrCuO}_2$  [12]) tend to become localized due to small random potentials, and hence may take the same role as static vacancies. If the impurities enter the chain in a completely random manner, the lengths of the chain segments thereby created follow a distribution function

$$P(l) = \rho \exp(-\rho l), \quad (4)$$

where  $\rho$  is the concentration of impurities per lattice site ( $0 < \rho < 1$ ). [13] Note that  $P(l)$  is properly normalized, and that its  $n^{\text{th}}$  moment is given by  $\langle l^n \rangle = n!/\rho^n$ . As illustrated in Fig. 2(a),  $P(l)$  is weighted towards smaller segments, with a maximum at  $P(0) = \rho$ . Thus for large impurity concentrations, the average over chain segments is dominated by contributions from the smaller clusters. On the other hand, in the dilute limit ( $\rho \ll 1$ )  $P(l)$  becomes flatter, and thus larger segments contribute appreciably to the average.

The average dynamical structure factor can consequently be calculated from

$$S(\pi, \omega) = \sum_l P(l) S(\pi, \omega, l), \quad (5)$$

where the sum is taken over all contributing chain segments with a non-vanishing Fourier component at  $q=\pi$ . In the case of large impurity concentrations, this sum may be cut off beyond a certain cluster length  $l_{\text{max}}$ , because the contributions of segments with  $l > l_{\text{max}}$  are exponentially suppressed by  $P(l)$ . Therefore, as long as  $l_{\text{max}}$  is smaller than the maximum cluster which can be studied with present computer capacities ( $\leq 36$  for

Heisenberg systems), very high accuracy can be achieved by simply taking the sum in Eq. 5 over all available finite systems. However, in the dilute impurity limit this procedure will necessarily break down, and we propose to use instead the fits obtained in Eqs. 1 and 2. [14]

To estimate the quality of such a few-pole approximation, we compare the spectrum  $S(\pi, \omega)$  obtained from cluster diagonalizations (Fig. 2(b)) at a rather large impurity concentration ( $\rho=0.3$ ), where  $l_{\text{max}} < 24$  and this procedure is most reliable, with that of a three-pole approximation using Eqs. 1 and 2 and extending the sum in Eq. 5 up to  $l = 10000$  (Fig. 2(c)). As can be seen by comparing the figures, the agreement between these two methods is very good for large  $\rho$ : the integrated spectral weight differs less than 0.5% at  $\rho=0.3$ . However, in the dilute impurity limit the three-pole approximation does account for the spectral weight due to the larger segments, yielding for example 14% more integrated intensity than the finite cluster average with  $l = 4, \dots, 24$  at  $\rho=0.1$ . In the following, when discussing the evolution of the dynamical spin structure factor with impurity doping, we will thus use the few-pole procedure rather than the average over system sizes available to exact diagonalization calculations.

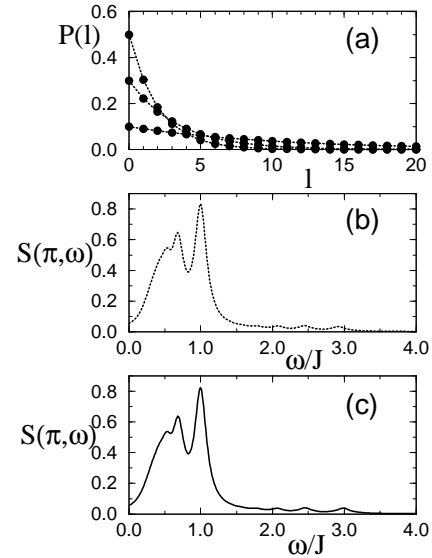


FIG. 2. (a) Distribution function of chain segments in a one-dimensional system with randomly placed non-magnetic impurities.  $P(l)$  is shown for impurity concentrations  $\rho = 0.1, 0.3$ , and  $0.5$ . (b) Dynamical structure factor at  $q=\pi$  for an antiferromagnetic spin-1/2 Heisenberg chain with  $\rho = 0.3$ , calculated from an average over finite cluster spectra with  $l = 4, \dots, 24$ . (c) Same as (b), but calculated using a three-pole approximation.

In Fig. 3 the evolution of  $S(\pi, \omega)$  is shown as a function of  $\rho$ . There are three main features that occur in  $S(\pi, \omega)$  upon randomly introducing vacancies into the chain: (i) the integrated spectral weight decreases rapidly with increasing  $\rho$ , (ii) a pseudo-gap develops at small frequencies, (iii) at larger frequencies (of order  $J$ ) a discrete peak

structure emerges, dominated by the contributions of the smallest cluster segments.

In order to discuss the low-energy features (i) and (ii), it is useful to consider the continuum limit of Eq. 5 since they are dominated by the contributions of the larger chain segments. We emphasize, however, that the discreteness of the peak structure at higher energies - which we consider to be a major characteristic - cannot be accounted for in this limit. For simplicity let us consider the single-pole approximation to leading order, i.e.  $\omega_1(l) = \alpha_1/l$  and  $A_1(l) = b_1 \ln(1+l)$  (for the weight of the lowest pole:  $a_1 = 0$ ). Replacing the sum in Eq. 5 with an integral it is then found that

$$S(\pi, \omega) \approx \frac{b_1 \alpha_1 \rho}{\omega^2} \ln\left(1 + \frac{\alpha_1}{\omega}\right) \exp\left(\frac{-\alpha_1 \rho}{\omega}\right), \quad (\omega \ll J). \quad (6)$$

Hence at low energies  $S(\pi, \omega)$  is exponentially suppressed, and the peak of the corresponding pseudo-gap feature moves towards larger frequencies with increasing  $\rho$ . The frequency sum-rule in the single-pole approximation yields  $S(\pi) = \int d\omega S(\pi, \omega) \approx b_1 \exp(\rho) E_1(\rho)$ , where  $E_1(\rho)$  is the first exponential integral. This result is in good agreement with the  $\rho$ -dependence of the frequency-integrated spectral weight obtained within the full three-pole approximation shown in Fig. 4(a).

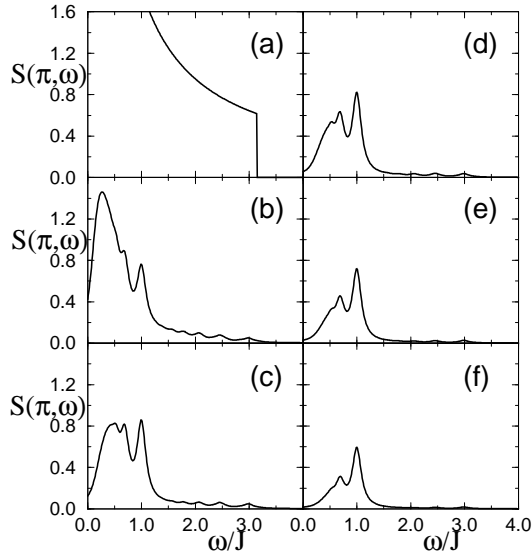


FIG. 3. Evolution of  $S(\pi, \omega)$  in the antiferromagnetic spin-1/2 Heisenberg chain as a function of impurity concentration, calculated from a three-pole approximation. In (a)-(f) the respective spectra are shown for  $\rho=0.0, 0.1, 0.2, 0.3, 0.4$ , and  $0.5$ .

From Eq. 6 it is seen that, strictly speaking, there should be no spectral weight at  $\omega = 0$ . However, if the  $\delta$ -peaks in Eq. 3 are given a finite lifetime, i.e. by replacing them with Lorentzians of width  $\epsilon$  in order to mimic the experimental situation, there will be some residual spinon density of states  $S(\pi, 0)$ . As shown in Fig. 4(b), this quantity is exponentially suppressed with increasing  $\rho$ , and it diverges in the dilute impurity limit.

According to our interpretation of the pseudo-gap by taking the continuum limit (Eq. 6), it arises due to the exponentially suppressed contributions of the largest segments (corresponding to the smallest finite-size gaps) to the average in Eq. 5. On the other hand, at higher energies ( $\omega \approx J$ ) the discrete nature of the smaller contributing clusters should be visible, with the largest features coming from the smallest clusters. Clearly, the lowest pole of the smallest contributing cluster at  $\omega = J$  is well defined in Figs. 3(b)-(f), advancing into the dominating feature of the spectrum for large  $\rho$ . At smaller impurity concentrations (Figs. 3 (b)-(d)) the lowest pole of the second smallest cluster is also well separated from the low-energy continuum. At larger  $\rho$ , however, it merges into the low-energy pseudo-branch. Summarizing the results for  $S(\pi, \omega)$  in the presence of randomly placed static vacancies, an inelastic neutron scattering experiment on such a system should observe a marked decrease of spectral weight with increasing impurity concentration, a low-energy pseudo-gap feature, and - resolution permitting - some split-off “high-energy” peaks due to (and indicating the size of) the smallest segments contributing to the average.

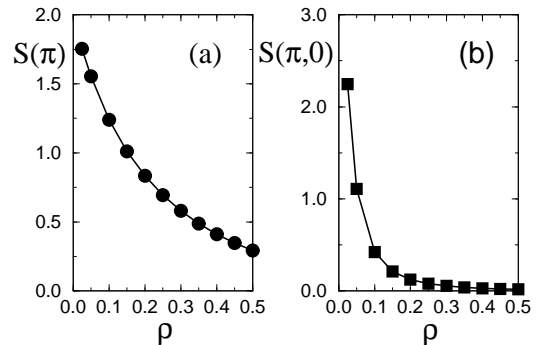


FIG. 4. (a) Dependence of the frequency-integrated dynamical structure factor at wavevector  $\pi$  on the concentration of non-magnetic impurities. (b) Residual spinon density of states as a function of impurity concentration.

In real materials, impurities do not necessarily enter a chain in an entirely uncorrelated manner, but may e.g. due to a lattice potential commensurate with the surrounding crystal structure favor certain distances between impurity sites. Effects of this kind can be accounted for by refining the probability distribution function in the above analysis. E.g. in the presence of a single preferred segment size  $l_0$  one finds

$$P(l) = \frac{\rho}{2 - \exp(-\rho l_0)} \exp(-|l - l_0|\rho), \quad (7)$$

which is peaked at  $l = l_0$ , and hence weighs the contribution by segments of length  $l_0$  most highly in the average. A spectral analysis of inelastic neutron scattering experiments on impurity doped systems can thus indicate the underlying distribution function of chain segments. In particular, at large  $\rho$  the characteristic “high-energy”

features coming from the segments with length  $l_0$  should dominate the spectral weight.

Odd-site segments do not contribute to the dynamical structure factor at  $q = \pi$ , but they have spectral weight at other momentum transfers which are contained in their Fourier spectrum. While even-site segments have a singlet ground state associated with a gap in their excitation spectrum, odd-site segments have a doublet ground state, and the effective low-energy spin-1/2 degree of freedom in these clusters leads to a single-spinon contribution to  $S(q, \omega)$  at small frequencies. This low-energy spectral weight from wavevectors close to  $\pi$  may “spill over”, causing a slight enhancement of the zero-frequency spinon density of states  $S(\pi, 0)$ . [15]

If there are residual inter-chain exchange couplings  $J_\perp$  ( $|J_\perp| \ll |J|$ ) in a quasi-one-dimensional magnetic material, there is a transition to a three-dimensional ordered phase at a low temperature  $T_N \sim |J_\perp|$ . [16] However, in the presence of an impurity-induced pseudo-gap in the chain spectrum,  $S(\pi, 0)$  does not diverge anymore at low temperatures, and thus  $T_N$  is decreased with increasing  $\rho$ . In the case of a vanishing residual spinon density of states this transition is completely suppressed, as it is the case for example in weakly coupled two-leg Heisenberg ladders. [17] In this sense impurities may have a stabilizing effect on one-dimensional phases. [18]

As a consequence of the spin-charge separation in one-dimensional systems away from half-filling, the spin and charge degrees of freedom can be treated equivalently. Therefore it can be expected for a segmented chain with (non-localized) mobile charge carriers that the results obtained above for  $S(q, \omega)$  hold also for the dynamical charge response  $N(q, \omega)$ .

To conclude, we have proposed an averaging procedure to account for the spectral features of one-dimensional systems in the presence of non-magnetic impurities. At small doping concentrations, the contributions of the longer segments become increasingly important, and the average over their lowest poles yields a pseudo-gap feature in the spin excitation spectrum at low frequencies. At larger impurity concentrations, the spectrum is dominated by discrete peaks at  $\omega \sim J$  contributed by the shortest segments.

When static vacancies are present in a correlated one-dimensional system, the formation of a pseudo-gap as discussed above will compete or coexist with other low-energy features, such as gaps due to frustrating exchange interactions or spin-Peierls instabilities. [19–22] In such systems it then remains to decide how much of the observed discrete low-frequency peak structure is due to such bulk instabilities or maybe to finite segment contributions. [23]

We wish to thank A. V. Balatsky, E. Dagotto, N. Furukawa, M. Laukamp, F. Mila, T. M. Rice, and M. Sigrist for useful discussions, and acknowledge the Swiss National Science Foundation for financial support.

- 
- [1] E. Abrahams, P. W. Anderson, D. C. Licciardello, and T. V. Ramakrishnan, Phys. Rev. Lett. **42**, 673 (1997).
  - [2] C. Kim *et al.*, Phys. Rev. Lett. **77**, 4054 (1996).
  - [3] M. Isobe and Y. Ueda, J. Phys. Soc. Jpn. **65**, 1178 (1996).
  - [4] D. A. Tennant *et al.*, Phys. Rev. Lett. **70**, 4003 (1993); D. A. Tennant *et al.*, Phys. Rev. B **52**, 13368 (1995); *ibid* 13381 (1995).
  - [5] J. des Cloiseaux and J. J. Pearson, Phys. Rev. **128**, 2131 (1962).
  - [6] G. Müller, H. Thomas, M. W. Puga, and H. Beck, J. Phys. C Solid State Phys. **14**, 3399 (1981).
  - [7] A. Fledderjohann, M. Karbach, K. H. Mütter, and P. Wielath, J. Phys.: Condensed Matter **7**, 8993 (1995); cond-mat/9609101.
  - [8] Note that the spectra shown in Fig. 1(a) were obtained on chains with periodic boundary conditions and an even number of sites. However, a Fourier analysis of the equivalent systems with open boundary conditions yields similar spectra with the same scaling behavior.
  - [9] I. Affleck, D. Gepner, H. J. Schulz, and T. Ziman, J. Phys. A: Math. Gen. **22**, 511 (1989).
  - [10] F. C. Alcaraz, M. N. Barber, and M. T. Batchelor, Phys. Rev. Lett. **58**, 771 (1987); F. C. Alcaraz and M. J. Martins, Phys. Rev. Lett. **61**, 1529 (1988).
  - [11] K. Nomura, Phys. Rev. B **48**, 16814 (1993).
  - [12]  $\text{La}^{3+}$  substitution for  $\text{Sr}^{2+}$  would actually donate an additional electron to the system. However, the electron could combine with one of the  $\text{Cu}^{2+}$  to form a singlet which acts as an effective hole in the chain.
  - [13] see e.g. M. Laukamp *et al.*, cond-mat/9707261. Note that strictly speaking the continuous function  $P(l)$  given by Eq. 4 is valid only in the dilute impurity limit and should be replaced by an equivalent discrete form for larger  $\rho$ .
  - [14] Although only a finite number of poles may be included in such a calculation, the dominant, low-energy contributions arise from the lowest few poles, and are thus accounted for to high accuracy.
  - [15] Odd-site segments also contribute multi-spinon spectral weight at wavevectors close to  $\pi$  and frequencies  $\omega \sim O(1/l)$ . These contributions can be treated analogously to those of the even-site segments.
  - [16] H. J. Schulz, Phys. Rev. Lett. **77**, 2790 (1996).
  - [17] M. Azuma *et al.*, Phys. Rev. Lett. **73**, 3463 (1994).
  - [18] At all impurity concentrations, the low-energy contributions to the spectral weight of the odd-site segments may lead to a small but finite  $T_N$ .
  - [19] G. S. Uhrig, Phys. Rev. Lett. **79**, 164 (1997); G. S. Uhrig and H. J. Schulz, Phys. Rev. B **54**, R9624 (1996).
  - [20] S. Haas and E. Dagotto, Phys. Rev. B **52**, R14396 (1995).
  - [21] M. Ain *et al.*, Phys. Rev. Lett. **78**, 1560 (1997).
  - [22] M. Arai *et al.*, Phys. Rev. Lett. **77**, 3649 (1996).
  - [23] The discrepancy of the broad measured static spin structure factor  $S(q)$  in  $\text{CuGeO}_3$  [22] and theoretical predictions [6,20] may originate in a random segmentation of the ideally infinite  $\text{CuO}_2$  chains in this material.